Analytical Techniques

XRF Major element analysis

Samples were ground in an agate mill to avoid any possible trace element contamination. Major element analyses were performed at the School of Earth Sciences (UTAS) using X-ray fluorescence spectrometry (XRF) and the methods of *Robinson et al.* [2003]. Whole rock sample powders were fused with 12-22 flux (a pre-fused mixture consisting of 12 parts $Li_2B_4O_7$ and 22 parts $LiBO_2$) using a sample:flux ratio of 1:9 at 1100˚C. All fusions are performed in a non-wetting 5% Au- 95% Pt alloy crucible. The following quantities are used to make 32mm diameter discs: - 12-22flux (4.5000g), sample (0.5000g) and $LiNO_3$ (0.0606g, added as 100µl of 60.6% $LiNO_3$). The mix is fused with agitation at 1100˚C for 15 minutes before being cast in a 5% Au -95% Pt mould. Ignition loss was determined on ~2 grams of sample powder ignited overnight at 1000˚C in 5ml platinum crucibles. Major elements were determined with a ScMo 3kW side window X-ray tube and a Philips PW1480 x-ray spectrometer. Corrections for mass absorption are calculated using Philips X40 software with De Jongh's calibration model and Philips (or CSIRO) alpha coefficients. Compton scattering is also used for many trace elements (see below). Calibrations are on pure element oxide mixes in pure silica, along with international and Tasmanian standard rocks are used.

XRF Trace element analysis

Trace element analyses (Rb, Ba, Nb, Sr, Zr, Y, V, Sc, Cr, Ni) were determined by using pressed powder pill analysis (10grams, 32mm) using a combination of ScMo (Y, Rb, Ni) and Au (Ba, Nb, Sr, Zr, V, Sc, Cr) 3kW side window X-ray tubes and a Philips PW1480 x-ray spectrometer.

ICP-MS Trace element analysis

ICP-MS trace element analyses at UTAS were obtained using the methods of *Robinson et al.* [1999] and *Yu et al.* [2000]. ICP-MS analyses were performed on duplicate high-pressure HF-$HClO_4$ digestions. Sub-boiling double distilled acids and ultra pure water were used, as were clean sampler and skimmer cones, ICP torch, spray chamber, nebuliser and sample introduction tubes (including auto-sampler tubing). Prior to sample analysis the instrument was purged for at least 24 hours with 5% v/v HNO_3 and 0.05% v/v HF rinse solution.

Sr-Nd-Pb isotopes

Hand-picked rock chips were acid washed in hot 6N HCl for 15 minutes and then dissolved in HF/HNO_3 acids. After extraction of Pb using conventional anion exchange using HBr-HCl media, Sr and LREE were extracted on EICHROM Sr. resin and RE.resin, respectively, followed by Nd purification on EICHROM LN resin [*Pin et al.,* 1994; *Pin and Santos-Zalduegui,* 1997]. Total procedural blanks were negligible in all cases with Pb blanks typically less than 20 pg.

All isotopic analyses were carried out on a Nu Instruments multi-collector ICP-MS coupled to a CETAC Aridus desolvating nebulizer [*Belshaw et al.,* 1998; Woodhead, 2002]. Instrumental mass bias was corrected by normalizing to $^{146}Nd/^{145}Nd$ = 2.0719425 (equivalent to $^{146}Nd/^{144}Nd$ = 0.7219, [*Vance and Thirlwall*, 2002]) and $^{86}Sr/^{88}Sr$ = 0.1194, using the exponential law. Further details can be found in *Maas et al.* [2005]. In the case of MC-ICPMS data, where mass bias is generally highly constant during a given analytical session, but can vary between sessions, data are routinely normalised to the standards of the day. In this case, data are reported relative to La Jolla Nd = 0.511860 and SRM987 = 0.710230. This secondary normalization yields the following results for international standards (±2sd): BCR-1 = 0.512641±18, BHVO-1 = 0.512998±18, JNdi-1 = 0.512113±22; E&A Sr carbonate = 0.708005±47, BCR-1 = 0.705016±46, BHVO-1 = 0.703478±36. These results compare well with data based on TIMS and MC-ICPMS from other laboratories (e.g. [*Raczek et al*., 2003; *Tanaka et al*., 2000]). Typical in-run precisions (2se) are ±0.000010 (Nd) and ±0.000022 (Sr). External (2sd) precision, or reproducibility, is ±0.000020 (Nd) and ±0.000040 (Sr) and is based on the results for secondary standards. Mass bias for Pb was corrected using the thallium-doping technique [*Woodhead*, 2002]. This produces data accurate to <±0.02% (with respect to the SRM981 Pb standard), with an external (2sd) precision of ≈±0.02%.

References

Belshaw, N.S., P.A. Freedman, R.K. O'Nions, M. Frank, and Y. Guo (1998), A new variable dispersion double-focusing plasma mass spectrometer with performance illustrated for Pb isotopes. *International Journal of Mass Spectrometry and Ion Processes,* 181, 51-58.

Maas, R., M.B. Kamenetsky, A.V. Sobolev, V. S. Kamenetsky, and N.V. Sobolev (2005), Sr-Nd-Pb isotopic evidence for a mantle origin of alkali chlorides and carbonates in the Udachnaya kimberlite, Siberia. *Geology*, 35, 549-552

Pin, C., D. Briot, C. Bassin, and F. Poitrasson (1994), Concomitant separation of strontium and samarium-neodymium for isotopic analysis in silicate samples, based on specific extraction chromatography. *Analytica Chimica Acta*, 298, 209-217.

Pin, C., and J. F. Santos-Zalduegui (1997), Sequential separation of light rare-earth elements, thorium and uranium by miniaturized extraction chromatography: application to isotopic analyses of silicate rocks. *Analytica Chimica Acta*, 339, 79-89.

Raczek, I., K. P. Jochum, and A. W. Hofmann (2003), Neodymium and strontium isotope data for USGS reference materials BCR-1, BCR-2, BHVO-1, BHVO-2, AGV-1, AGV-2, GSP-1, GSP-2 and eight MPI-DING reference glasses. *Geostandards Newsletter*, 27, 173-179

Robinson, P. (2003), XRF analysis of flux-fused discs, Geoanalysis 2003, *The 5th International Conference on the Analysis of Geological and Environmental Materials, Abstracts*, 90.

Robinson, P., A. T. Townsend, Z. Yu, and C. Munker (1999), Determination of Scandium, Yttrium and Rare Earth Elements in rocks by high resolution inductively coupled plasma-mass spectrometry, *Geostandards Newsletter, 23*, 31-46.

Tanaka, T., and 18 others (2000), JNdi-1: a neodymium isotopic reference in consistency with La Jolla neodymium. *Chemical Geology*, 168, 279-281.

Vance, D., and M. F. Thirlwall (2002), An assessment of mass discrimination in MC-ICPMS using Nd isotopes. *Chemical Geology*, 185, 227-240.

Woodhead, J.D. (2002), A simple method for obtaining highly accurate Pb isotope data by MC-ICP-MS. *Journal of Analytical Atomic Spectrometry*, 17, 1-6

Yu Z., P. Robinson, A. T. Townsend, C. Munker, and A. J. Crawford (2000), Determination of HFSE, Rb, Sr, Mo, Sb, Cs, Tl and Bi at ng g-1 levels in geological reference materials by magnetic sector ICP-MS after HF/HCLO4 high pressure digestion, *Geostandards Newsletter, 24*, 39-50.

GEOLOGICAL SETTING

The Kadavu Island Group (Figure S1) lies approximately 88 km south of the main Fijian Island of Viti Levu in the southwest Pacific. It forms the northernmost and emergent part of the submarine Hunter Ridge, and is separated from the main Fijian Platform (defined by an area of shallow water, generally less than 1 km deep), upon which the major Fiji islands are located (Colley and Hindle, 1984; Rodda, 1994) by the relatively deep water (2000-2500m) of the Kadavu Channel. The Kadavu Trench lies between Kadavu Island and seafloor of the South Fiji Basin.

The submarine Hunter Ridge forms the south-eastern boundary of the North Fiji Basin, linking the southern end of the Vanuatu Arc with the Fiji Platform. It is part of the tectonically complex New Hebrides-Fiji Orogen (Bird, 2003). The number and nature of plate boundaries in this area is poorly defined (Bird, 2003). The Hunter Ridge is a series of submarine ridges, associated in part with large sinistral earthquakes, that separates the actively spreading North Fiji Basin from the extinct South Fiji Basin. It is not clear whether it forms part of a plate boundary or not (Bird, 2003). Auzende et al. (1996) proposed that the Hunter Ridge was an embryonic island arc formed during a short period (~7-3Ma) of north-directed subduction of the South Fiji Basin oceanic crust under the North Fiji Basin and Fiji Platform. The Kadavu Trench was formed as a result of this process. The development of this arc was aborted when northward subduction ceased due to plate reorganisation. Presently, there is no evidence for active arc volcanoes on the Hunter Ridge, apart from those occurring within an active rift at the southern end of the Hunter Ridge (Danyushevsky et al. 2006) where the main N-S orientated spreading centre of the North Fiji Basin is transecting the Hunter Ridge. Limited sampling of the Hunter Ridge to the southwest of Kadavu Island has recovered volcanics comprising a typical low-K island arc tholeiite suite (Verbeeten, 1996).

The volcanic rocks of the Kadavu Island Group range in age from 3.4 - 0.36 Ma (Figure S1, Whelan et al.,1985) and are the youngest subduction-related volcanism on the Fijian Islands. Kadavu is the only island within the Fiji archipelago where adakites have been described. Geological mapping by Woodrow (1980), and our fieldwork, demonstrates that the Kadavu Island Group is composed of a number of volcanic units forming three main volcanic groups that young from north to south. The oldest group (~3.4 Ma, Whelan et al., 1985) are the shoshonitic lavas forming the Astrolabe Islands. The youngest groups are the adakitic lavas of Eastern and Western Kadavu (~0.5-2.9 Ma; Whelan et al., 1985).

Shoshonitic magmatism in Fiji occurred from ~5.5 to 3.0 Ma (Whelan et al., 1985), with Astrolabe shoshonites being the youngest. The Astrolabe shoshonite lavas range from relatively primitive olivine + clinopyroxene - phyric absorakites (e.g. AV186, Table 1) to relatively more differentiated plagioclase + clinopyroxene + biotite + hornblende - phyric andesites. Their parental magmas probably represent relatively low degree partial melts of a refractory mantle source which had a previous history of enrichment by subduction zone fluids (Leslie, 2005). This source enrichment most likely took place during subduction at the paleo-Vitiaz trench. Post-subduction rifting and rotation of the Fiji Platform and surrounding areas since 5 Ma induced decompression melting of these enriched subduction modified mantle sources (Gill et al. 1984; Leslie, 2005).

The oldest adakite lavas occur in Eastern Kadavu and the small island of Ono (~2.8 Ma). The youngest adakite lavas occur in Western Kadavu (Figure S1) and consist of two subgroups. The first are HSA lavas, and the second are relatively primitive LSA lavas forming the small islet of Ngaloa (Figure S1) as well as isolated outcrops overlying the older adakites of Eastern Kadavu. Although the youngest age reported by Whelan et al. (1985) of 0.36 Ma is from Ngaloa Island, from the presence of magmatic enclaves of Ngaloa LSA within the Western Kadavu HSA lavas indicates that both the LSA magmas of Ngaloa and the

HSA magmas of Western Kadavu were erupting simultaneously. The HSA adakites from both the Eastern and Western Kadavu are andesitic to dacitic in composition and contain up to 60 vol% phenocrysts of plagioclase, clinopyroxene, hornblende, biotite and magnetite, with minor altered olivine (2-7 vol%) present in some of the more magnesian adakites from Western Kadavu (Verbeeten, 1996).

References:

Auzende, J.M., Pelletier, B. and Eissen J.P., 1996, The North Fiji Basin: geology, structure and geodynamic evolution: In, Taylor, B (ed). Backarc basins: tectonics and magmatism, Plenum Press, New York. pp. 139-175.

Bird, P., 2003, An updated digital model of plate boundaries: Geochemistry, Geophysics, Geosystems, v. 4, no. 3, doi:10.1029/2001GC000252.

Colley, H. and Hindle, W. H., 1984, Volcano-tectonic evolution of Fiji and adjoining marginal basins. In: Kokelaar, B.P. and Howells, M.F. (eds), Marginal Basin Geology: Geological Society of London, pp 151-162.

Danyushevsky, L.V., Falloon, T.J., and Crawford, A.J., 2006, Subduction-related magmatism at the southern tip of the North Fiji backarc basin: Extended Abstracts (CD), Australian Earth Sciences Convention 2006, 2–6 July 2006, Melbourne, Australia. 1–8.

Gill, J. B., Stork, A. L., and Whelan, P. M., 1984, Volcanism accompanying backarc basin development in the southwest Pacific: Tectonophysics, v. 102, p. 207-224.

Leslie, R.A.J., 2005, Primitive Shoshonites from Fiji: Mineralogy, Melt Inclusions and Geochemistry: Unpubl PhD thesis, UTAS, pp. 360.

Rhodda, P., 1994, Geology of Fiji. In, Stevenson, A. J., Herzer, R. H., and Balance, P. F. (eds), Geology and submarine resources of the Tonga Lau - Fiji Region. SOPAC Technical Bulletin, v. 8, p. 131-151.

Verbeeten, A., 1996, Petrology, Geochemistry and tectonic implications of magmatism along the northern Hunter Ridge and Kadavu Island group, Fiji: Unpubl PhD thesis, UTAS, pp. 190.

Whelan, P.M., Gill, J. B., Kollman, E., Duncan, R. A. & Drake, R. E., 1985, Radiometric dating of magmatic stages in Fiji: In: Scholl, D.W. & Vallier, T.L. (eds), Geology and offshore resources of Pacific island arcs - Tonga region. Circum-Pacific Council for Energy and Mineral Resources Earth Science Series, v.2. Houston, Texas.

Woodrow, P.J., 1980, Geology of Kadavu: Mineral Resources Department, Fiji, Bulletin no. 7.

Sample №	**Texture**	**Phenocrysts and microphenocrysts**	**Groundmass**
WESTERN KADAVU			
ST1	highly porphyritic	*plagioclase:* 35%, 0.5-5mm (some grains up to 12mm), subhedral-euhedral, oscillatory zoned. *hornblende:* 5%, 0.3-0.6mm, subhedral, opacitic rims. *biotite:* 2%, 0.2-0.9mm, subhedral, opacitic rims. *magnetite:* 2%, 0.05-0.2mm.	fine grained to glassy consisting of plagioclase microlites and magnetite.
ST5	highly porphyritic	*plagioclase:* 35%, 0.5-4mm (some grains up to 10mm), subhedral, oscillatory zoned. *hornblende:* 15%, 0.2-0.9mm (some grains up to 4mm), subhedral-euhedral, partially to totally replaced with magnetite. *biotite:* 7%, 0.4-2mm, subhedral, partially to totally replaced with magnetite. *clinopyroxene:* 3%, 0.2-0.6mm, subhedral-anhedral, sometimes in crystal clusters. *magnetite:* 1%, 0.05-0.1mm.	glassy containing plagioclase laths and magnetite, glass partially recrystallised.
ST14	highly porphyritic	*plagioclase:* 20%, 0.8-4mm, subhedral-euhedral, oscillatory zoned. *biotite:* 10%, 0.5-5mm, subhedral. *hornblende:* 7%, 0.2-1.5mm, subhedral-anhedral. *magnetite:* 3%, 0.1-0.2mm.	fine grained consisting of plagioclase microlites, magnetite and minor hornblende.
ST16	highly porphyritic	*plagioclase:* 60%, 0.3-2mm, subhedral-euhedral, zoned, sieve like texture *clinopyroxene:* 7%, 0.1-0.6mm, subhedral-anhedral, microphenocrysts only. *magnetite:* 3%, 0.05-0.2mm.	fine grained consisting of plagioclase needles and magnetite.
ST17	highly porphyritic	*plagioclase:* 60%, 0.3-2mm, subhedral-euhedral, strongly zoned, sieve like texture. *clinopyroxene:* 10%, 0.1-0.6mm, light-green, subhedral, sometimes in clusters with hornblende and magnetite.	fine grained consisting of plagioclase microlites and magnetite.

		hornblende: 1%, 0.1-0.4mm, subhedral, rarely zoned. *magnetite:* 2%, 0.05-0.2mm.	
ST18	porphyritic	*plagioclase:* 50%, 0.3-2mm, subhedral, oscillatory zoned. *clinopyroxene:* 10%, 0.1-0.6mm, subhedral-anhedral, contains inclusions of magnetite. *hornblende:* <1%, 0.1-0.4mm, subhedral, opacitic rims, contains inclusions of magnetite. *magnetite:* 3%, 0.05-0.1mm.	fine grained consisting of plagioclase laths, magnetite and rare clinopyroxene.
ST19	highly porphyritic	*plagioclase:* 50%, 0.3-2mm, subhedral-euhedral, strongly zoned, sieve like texture. *clinopyroxene:* 7%, 0.1-1.3mm, light-green, subhedral contains inclusions of magnetite. *hornblende:* 1%, 0.1-0.4mm, subhedral-anhedral, opacitic rims, contains inclusions of magnetite. *magnetite:* 3%, 0.05-0.1mm.	fine grained consisting of plagioclase laths, magnetite and rare clinopyroxene.
ST20	porphyritic	*plagioclase:* 30%, 0.4-3mm, subhedral-anhedral, zoned. *hornblende:* 15%, 0.1-1mm, subhedral, partially to totally replaced with magnetite (+hematite?). *biotite:* 10%, 0.2-1mm, subhedral, partially to totally replaced with magnetite (+hematite?) and chlorite. *clinopyroxene:* 4%, 0.05-0.3mm, microphenocrysts only, anhedral, mostly in crystal clusters, some grains partially resorbed. *magnetite:* 2%, 0.05-0.1mm.	grained consisting of plagioclase microlites and magnetite.
ST21	porphyritic	*plagioclase:* 25%, 0.3-2mm, subhedral, oscillatory zoned. *clinopyroxene:* 5%, 0.1-0.5mm, anhedral, contains inclusions of magnetite. *hornblende:* <1%, 0.1-0.4mm, subhedral-anhedral, few singular grains. *magnetite:* 3%, 0.05-0.1mm.	glassy containing plagioclase needles and magnetite, glass partially recrystallised, altered.
ST22	highly	*plagioclase:* 50%, 0.2-1mm, subhedral, oscillatory zoned.	glassy containing plagioclase

	porphyritic	*clinopyroxene:* 7%, 0.1-0.8mm, subhedral-anhedral, inclusions of magnetite. *magnetite:* 3%, 0.05-0.1mm.	laths and magnetite, glass recrystallised, altered.
ST23	porphyritic, vesicular	*plagioclase:* 20%, 0.3-1mm, subhedral-euhedral, strongly zoned. *clinopyroxene:* 10%, 0.2-1mm, subhedral-anhedral, contains inclusions of magnetite, partially resorbed. *magnetite:* 3%, 0.05-0.1mm.	fine grained to glassy consisting of plagioclase laths and magnetite, glass recrystallised, altered.
ST24	porphyritic, vesicular	*plagioclase:* 25%, 0.1-0.8mm, subhedral, partially altered. *clinopyroxene:* 7%, 0.1-0.8mm, anhedral, partially altered. *magnetite:* 3%, 0.05-0.1mm.	fine grained to glassy consisting of plagioclase microlites and magnetite, altered.
ST25	highly porphyritic	*plagioclase:* 50%, 0.2-1.5mm, subhedral-euhedral, oscillatory zoned. *clinopyroxene:* 10%, 0.1-1mm, subhedral-anhedral, contains inclusions of magnetite, some grains partially replaced with magnetite. *magnetite:* 3%, 0.05-0.1mm.	fine grained consisting of plagioclase microlites and magnetite.
ST26	porphyritic	*plagioclase:* 15%, 0.2-1mm, subhedral, strongly zoned, sieve like texture, inclusions of clinopyroxene. *clinopyroxene:* 20%, 0.1-1.5mm, subhedral-anhedral, zoned. *olivine:* 2%, 0.1-0.5mm, completely altered. *magnetite:* 2%, 0.05-0.1mm.	fine grained to glassy consisting of plagioclase laths, magnetite and rare clinopyroxene, glass recrystallised.
ST27	porphyritic	*plagioclase:* 15%, 0.2-1.5mm, subhedral, oscillatory zoned, sieve like texture. *clinopyroxene:* 15%, 0.1-1.5mm, subhedral-anhedral, zoned, some cores altered. *olivine:* 5%, 0.1-0.6mm, completely altered. *magnetite:* 2%, 0.05-0.2mm.	grained consisting of plagioclase microlites magnetite and clinopyroxene, altered.
ST28	highly porphyritic	*plagioclase:* 35%, 0.3-2mm, subhedral, zoned. *clinopyroxene:* 15%, 0.1-1.5mm, subhedral-euhedral, contains inclusions of magnetite.	grained consisting of plagioclase laths, magnetite and rare clinopyroxene.

		hornblende: 5%, 0.4-1.5mm, subhedral, partially replaced with magnetite. *magnetite:* 3%, 0.05-0.1mm.	
ST29	highly porphyritic	*plagioclase:* 50%, 0.2-2mm, subhedral-euhedral, strongly zoned, sieve like texture. *clinopyroxene:* 7%, 0.1-0.9mm, subhedral-euhedral, contains inclusions of magnetite. *magnetite:* 4%, 0.05-0.1mm.	fine grained consisting of plagioclase laths and magnetite.
ST31	porphyritic	*plagioclase:* 15%, 0.2-1.5mm, subhedral, oscillatory zoned. *clinopyroxene:* 15%, 0.1-1.5mm, subhedral, zoned, sieve like texture. *olivine:* 7%, 0.1-0.6mm, completely altered. *magnetite:* 2%, 0.05-0.2mm.	grained consisting of plagioclase microlites magnetite and clinopyroxene, altered.
EASTERN KADAVU			
ST43	porphyritic	*plagioclase:*<1%, 0.1-0.3mm, microphenocrysts only, subhedral. *clinopyroxene:* 10%, 0.1-1.5mm, subhedral, sometimes in clusters with olivine, two types – colourless, slightly altered, some cores with sieve like texture; grains with small bottle-green cores and colourless rims. *olivine:* 5%, 0.1-0.6mm, subhedral, resorbed, slightly altered. *magnetite:* 3%, 0.05-0.1mm.	grained consisting of plagioclase laths, clinopyroxene and magnetite.
ST44	porphyritic	*plagioclase:*<1%, 0.1-0.3mm, microphenocrysts only, subhedral. *clinopyroxene:* 10%, 0.1-1.2mm, subhedral, commonly in clusters with olivine, two types – colourless, slightly altered, slightly resorbed, some cores with sieve like texture; grains with small bottle-green cores and colourless rims. *olivine:* 5%, 0.1-0.8mm, subhedral, slightly altered. *magnetite:* 3%, 0.05-0.1mm.	grained consisting of plagioclase laths, clinopyroxene and magnetite.

NGALOA			
ST45	porphyritic, highly oxidised	*clinopyroxene:* 10%, 0.1-1.3mm, subhedral, three types – colourless, slightly altered; cores with sieve like texture, slightly resorbed; light- to bottle-green cores with colourless rims. *olivine:* 3%, 0.1-0.3mm, microphenocrysts only, subhedral, totally replaced with magnetite and iddingsite. *magnetite:* 3%, 0.05-0.1mm.	fine grained consisting of plagioclase laths, clinopyroxene and magnetite, altered (oxidised).
ST46	porphyritic, highly oxidised	*plagioclase:*<1%, 0.1-0.4mm, subhedral, strongly zoned. *clinopyroxene:* 7%, 0.1-0.9mm, subhedral, three types – colourless; cores with sieve like texture, slightly resorbed; bottle-green cores with colourless rims. *olivine:* 2%, 0.1-0.2mm, microphenocrysts only, subhedral-anhedral, partially altered to iddingsite. *magnetite:* 3%, 0.05-0.1mm.	fine grained consisting of plagioclase laths, clinopyroxene, magnetite and rare phlogopite needles, altered (oxidised).
ST47	porphyritic, highly oxidised	*clinopyroxene:* 10%, 0.1-0.9mm, subhedral, sometimes in crystal clusters, three types – colourless; cores with sieve like texture, slightly resorbed; bottle-green cores with colourless rims. *olivine:* 1%, 0.1-0.2mm, microphenocrysts only, subhedral-anhedral, magnetite rims, totally replaced with magnetite and iddingsite. *magnetite:* 5%, 0.05-0.1mm.	fine grained consisting of plagioclase laths, clinopyroxene, magnetite and rare phlogopite needles, altered (oxidised).
ST48	porphyritic, highly oxidised	*clinopyroxene:* 15%, 0.2-1.5mm, subhedral, three types – colourless, slightly altered; cores with sieve like texture, slightly resorbed; bottle-green cores (containing inclusions of magnetite) with colourless rims. *olivine:* 3%, 0.1-0.6mm, subhedral, slightly resorbed, inclusions of magnetite, slightly replaced with magnetite. *magnetite:* 5%, 0.05-0.1mm.	fine grained consisting of plagioclase laths, clinopyroxene and magnetite, altered (highly oxidised).
ST49	porphyritic,	*plagioclase:*<1%, 0.1-0.3mm, microphenocrysts only,	grained consisting of plagioclase

	highly oxidised	subhedral, zoned. *clinopyroxene:* 15%, 0.2-1.8mm, subhedral, some cores with sieve like texture, commonly in crystal aggregates, slightly resorbed. *olivine:* 1%, 0.1-0.2mm, microphenocrysts only, subhedral-anhedral, magnetite rims, slightly resorbed, slightly replaced with magnetite. *magnetite:* 5%, 0.05-0.1mm.	laths, clinopyroxene and magnetite, altered (highly oxidised).
NG1	porphyritic, oxidised	*clinopyroxene:* 10%, 0.2-2mm, subhedral, commonly in clusters with olivine and phlogopite, two types – colourless, cores usually with sieve like texture; rare grains with small bottle-green cores and colourless rims. *olivine:* 5%, 0.1-1mm, subhedral, slightly resorbed, slightly altered. *phlogopite:* 3%, 0.1-0.4mm, anhedral, contains inclusions of magnetite, commonly in clusters with olivine and clinopyroxene. *magnetite:* 5%, 0.05-0.1mm.	grained consisting of plagioclase laths, clinopyroxene, magnetite and rare phlogopite, altered (highly oxidised).
NG2	porphyritic, oxidised	*clinopyroxene:* 10%, 0.1-0.8mm, subhedral, zoned, some cores with sieve like texture, slightly resorbed, commonly in aggregates with olivine. *olivine:* 3%, 0.1-0.6mm, subhedral, slightly resorbed, altered to iddingsite with magnetite. *magnetite:* 5%, 0.05-0.1mm.	grained consisting of plagioclase laths, clinopyroxene and magnetite, altered (oxidised).
NG3	porphyritic, slightly oxidised	*clinopyroxene:* 10%, 0.2-1.3mm, subhedral, most cores with sieve like texture, slightly resorbed, commonly in clusters with olivine and phlogopite. *olivine:* 5%, 0.1-0.6mm, subhedral, slightly resorbed, magnetite rims, slightly altered. *phlogopite:* 2%, 0.1-0.2mm, anhedral, contains inclusions of magnetite, microphenocrysts only, commonly in clusters	grained consisting of plagioclase laths, clinopyroxene, magnetite and rare phlogopite, altered (slightly oxidised).

		with olivine and clinopyroxene. *magnetite:* 5%, 0.05-0.1mm.	
NG4	porphyritic, oxidised	*clinopyroxene:* 15%, 0.2-1.3mm, subhedral, commonly in clusters with olivine and phlogopite, two types – colourless, cores usually with sieve like texture; rare grains with small bottle-green cores and colourless rims. *olivine:* 1%, 0.1-0.3mm, microphenocrysts only, subhedral-anhedral, inclusions of magnetite, slightly altered. *phlogopite:* 2%, 0.1-0.2mm, anhedral, contains inclusions of magnetite, microphenocrysts only, commonly in clusters with olivine and clinopyroxene. *magnetite:* 5%, 0.05-0.1mm.	grained consisting of plagioclase laths, clinopyroxene and magnetite, altered (oxidised).

SUPPLEMENTARY DISCUSSION

Alternative possibilities for the high-SiO_2 rich end member on Kadavu, which we consider less likely, include a 'normal' evolved arc magma; high-pressure crystal fractionation of a 'normal' arc magma; and melting of the lower crust under the volcano.

Figure 3c and Figure S3 (supplementary materials) the Hunter Ridge island arc series volcanics have a restricted range of low Sr/Y (<25) and La/Yb (<2) similar to other well known island arc tholeiite series rocks such as the Tofua Arc, Tonga. Figure S3 (supplementary materials) demonstrates that crystal fractionation of a typical island arc tholeiite series basalt such as the Hunter ridge or Tongan islands produces magmas with a wide range of SiO_2 (~50-74 wt%) with slowly decreasing Sr/Y ratios (~25 decreasing to ~ <10 with SiO_2, see Figure S3). Mixing of an enriched high-Mg adakite such as the East Kadavu end-member, combined with crystal fractionation, could potentially produce a wide range of magmas with elevated Sr/Y similar to the Kadavu adakites. However, this model cannot reproduce other important features of the low-Mg Kadavu adakites, such as high La/Yb values (Figure 3c). In contrast, mixing with slab melts can explain the observed range of Kadavu adakite compositions.

High-pressure fractionation of normal arc magmas has recently been suggested as a general model for adakite genesis (Macpherson et al., 2006). Although this model can explain the trace element features of adakites, it is not consistent with the observed order of crystallisation of calc-alkaline and tholeiitic series at high pressure. Experimental studies (Müntener et al., 2001; Green, 1992) and detailed petrology of calc-alkaline suites where there is clear evidence for high-pressure fractionation (Day et al., 1992) demonstrate that garnet is a late fractionating phase, and thus can only produce modest increases in Sr/Y ratio. For example, the Miocene calc-alkaline suite from Northland, New Zealand (Day et al., 1992) ranges from basaltic andesite with Sr/Y of ~ 5 to rhyolites with Sr/Y ~50 (see Figure S3, supplementary data). The crystallization sequence involves extensive olivine fractionation from a hydrous arc basalt before fractionation involving clinopyroxene, orthopyroxene and amphibole, leading eventually to plagioclase and garnet becoming fractionating phases. This sequence is similar to those obtained in high-pressure experimental studies (Müntener et al., 2001; Green, 1992) and results in CIPW corundum normative liquids at ~60 wt% SiO_2 and the presence of garnet phenocrysts in dacites and rhyolites (Day et al., 1992). The Kadavu adakites are not CIPW corundum normative, they lack garnet phenocrysts and have significantly higher Sr/Y ratios than can be achieved by high-pressure crystal fractionation of normal arc basalts (see Figure S3, supplementary data).

As the Kadavu adakite magma series is erupted onto a basement formed by Hunter Ridge arc crust (Holmes et al., 1985), it is conceivable that the SiO_2 rich end-member is a melt from lower crustal cumulates. We consider that this possibility is less likely based on studies of oceanic gabbros (Nonnotte et al., 2005; Koepke et al., 2007) which demonstrate that oceanic crustal melts do not have adakite compositions.

References

Day, R. A., Green, T. H., and Smith, I. E. M., 1992, The origin and significance of garnet phenocrysts and garnet-bearing xenoliths in Miocene calc-alkaline volcanics from Northland, New Zealand: Journal of Petrology, v. 33, p. 125-161.

Green, T. H., 1992, Experimental phase equilibrium studies of garnet-bearing I-type volcanics and high-level intrusives from Northland, New Zealand: Transactions of the Royal Society of Edinburgh: Earth Sciences, v. 83, p. 429-438.

Holmes, R., Prasad, A., Honza, E., 1985, Seismic profiles from the Fiji area: In, Honza, E., Lewis, K.B., and Shipboard Party, A Marine Geological and Geophysical Survey of the Northern Tonga Ridge and Adjacent Lau Basin, Ministry of Lands, Survey and Natural Resources, Kingdom of Tonga, Field Report no.1, p. 37-41.

Koepke, J., Berndt, J., Feig, S. T., and Holtz, F., 2007, The formation of SiO2-rich melts within the deep oceanic crust by hydrous partial melting of gabbros: Contributions to Mineralogy and Petrology, v. 153, p. 67–84, doi: 10.1007/s00410-006-0135-y.

Macpherson, C.G., Dreher, S.T., and Thirlwall, M.F., 2006, Adakites without slab melting: High presure differentiation of island arc magma, Mindanao, the Philippines: Earth and Planetary Science Letters, v. 243, p. 581–593, doi: 10.1016/j.epsl.2005.12.034.

Müntener, O., Kelemen, P. B., and Grove, T. L., 2001, The role of H_2O during crystallization of primitive arc magmas under uppermost mantle conditions and genesis of igneous pyroxenites: an experimental study: Contributions to Mineralogy and Petrology, v. 141, p. 643-658.

Nonnotte, P., Ceuleneer, G., and Benoit, M., 2005, Genesis of andesitic-boninitic magmas at mid-ocean ridges by melting of hydrated peridotites: Geochemical evidence from DSDP Site 334 gabbronorites: Earth and Planetary Science Letters, v. 236, p. 632-653.

DR2008118

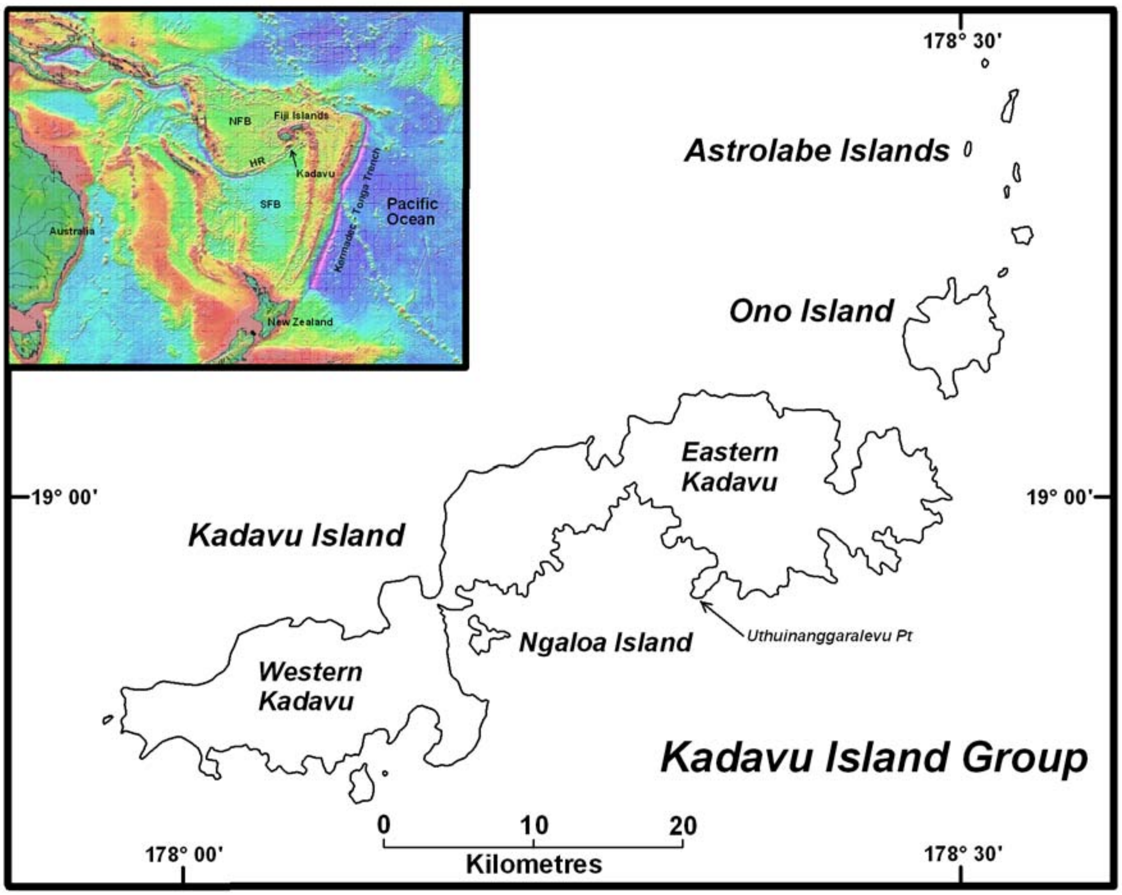
NFB
Fiji Islands
HR
Kadavu
SFB
Australia
Kermadec - Tonga Trench
Pacific Ocean
New Zealand
178° 30'
Astrolabe Islands
Ono Island
Eastern Kadavu
19° 00'
19° 00'
Kadavu Island
Uthuinanggaralevu Pt
Ngaloa Island
Western Kadavu
Kadavu Island Group
0
10
20
Kilometres
178° 00'
178° 30'

DR2008118

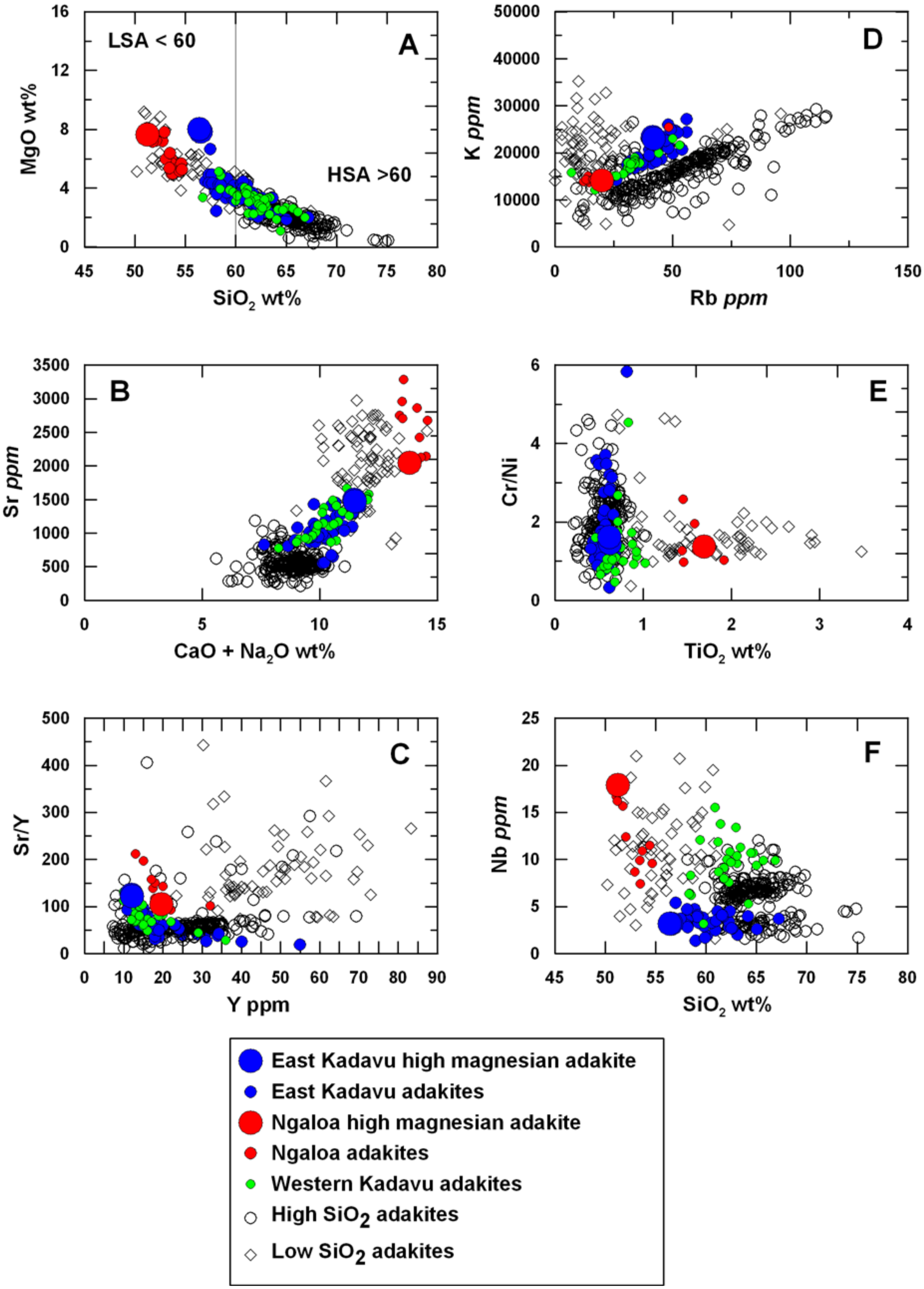
A
LSA < 60
HSA >60
MgO wt%
SiO_2 wt%
D
K *ppm*
Rb *ppm*
B
Sr *ppm*
CaO + Na_2O wt%
E
Cr/Ni
TiO_2 wt%
C
Sr/Y
Y ppm
F
Nb *ppm*
SiO_2 wt%
East Kadavu high magnesian adakite
East Kadavu adakites
Ngaloa high magnesian adakite
Ngaloa adakites
Western Kadavu adakites
High SiO_2 adakites
Low SiO_2 adakites

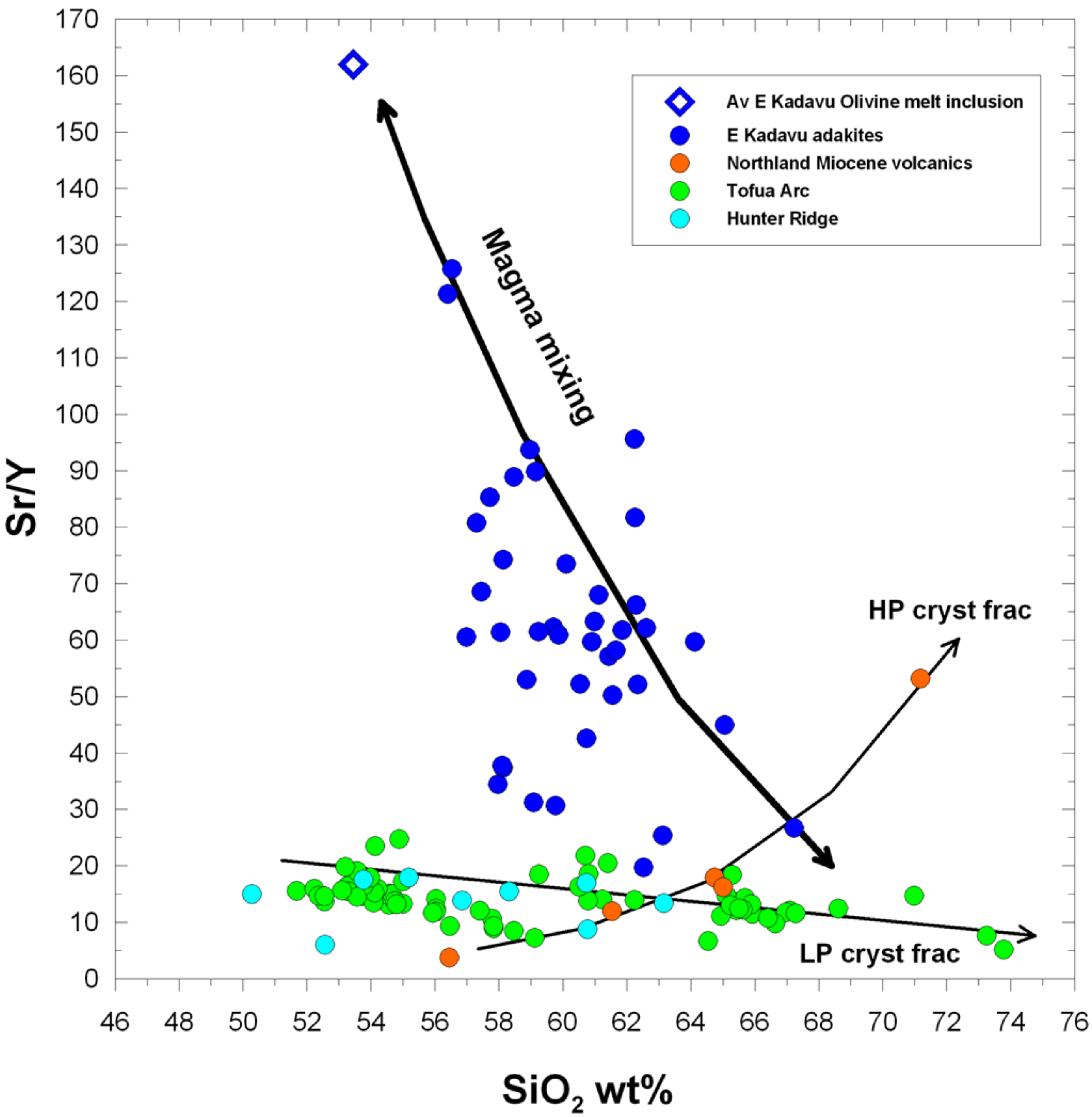
Av E Kadavu Olivine melt inclusion
E Kadavu adakites
Northland Miocene volcanics
Tofua Arc
Hunter Ridge
Magma mixing
HP cryst frac
LP cryst frac
Sr/Y
SiO2 wt%
170
160
150
140
130
120
110
100
90
80
70
60
50
40
30
20
10
0
46
48
50
52
54
56
58
60
62
64
66
68
70
72
74
76

Sample no.	Description	Lat	Long	SiO2	TiO2	Al2O3	FeOT
AV37	lava flow	19 04.2	178 03.9	60.85	0.87	15.96	4.41
AV84	lava flow	19 09.3	178 10.3	58.43	0.83	17.13	5.97
AV54	lava flow	19 08.9	178 01.2	59.37	1.02	16.57	4.73
AV70	lava flow	19 10.8	178 06.7	61.16	0.93	16.67	4.43
AV78	lava flow	19 08.3	178 11.2	59.74	0.52	17.73	5.63
AV76	float in creek	19 07.1	178 08.4	61.80	0.69	16.67	4.60
AV77	lava flow	19 08.0	178 07.3	61.42	0.92	16.19	4.59
AV48	lava flow	19 08.9	177 58.4	63.39	0.89	15.84	3.69
AV72	lava flow	19 07.8	178 04.8	62.37	0.77	16.50	4.42
AV62	lava flow	19 08	178 03.2	62.04	0.63	16.97	4.18
AV73	lava flow	19 06.2	178 04.2	63.06	0.68	16.98	3.93
AV85	lava flow	19 07.9	178 09.3	62.93	0.74	16.58	3.97
AV91	lava flow	19 07.0	178 11.3	62.26	0.59	17.35	4.56
AV94	lava flow	19 04.0	178 09.4	63.05	0.64	17.18	4.09
AV14	lava flow	19 06.7	177 58.1	64.98	0.55	16.35	3.28
AV50	float in creek	19 07.8	177 59.0	65.66	0.60	16.18	3.35
AV40	float in creek	19 05.3	178 01.7	64.17	0.52	17.69	3.39
AV5	lava flow	19 02.7	178 08.8	64.69	0.58	16.76	3.48
AV66	float on beach	19 09.7	178 03.8	62.46	0.68	17.69	3.94
AV57	lava flow	19 08.7	178 02.5	61.21	0.88	17.68	4.51
AV59	lava flow	19 08.3	178 02.4	61.76	0.65	18.36	4.02
AV90	lava flow	19 07.0	178 11.4	66.87	0.46	16.18	3.16
AV31	clast in breccia	19 04.9	178 07.0	64.44	0.70	17.57	4.27
ST1	lava flow	19 07.8	177 58.4	66.17	0.48	16.54	2.94
ST5	lava flow	19 06.7	177 57.8	60.94	0.96	16.36	4.33
ST14	lava flow	19 06.4	177 59.2	63.10	0.75	16.66	3.39
ST16	float on beach	19 04.5	178 02.5	64.05	0.52	17.82	3.60
ST17	float on beach	19 04.5	178 02.5	62.95	0.58	17.60	3.71
ST18	float on beach	19 04.5	178 02.5	62.88	0.61	17.23	3.79
ST19	float on beach	19 04.5	178 02.5	62.44	0.72	17.58	3.88
ST20	lava flow	19 00.2	178 01.8	63.32	0.81	16.45	4.19
ST21	lava flow	19 00.2	178 01.8	61.50	0.65	18.19	3.77
ST22	lava flow	19 09.5	178 09.5	61.27	0.49	17.54	5.01
ST23	clast in breccia	19 09.5	178 09.5	60.17	0.54	17.77	5.14
ST24	clast in breccia	19 09.5	178 09.5	59.97	0.55	18.40	5.14
ST25	float on beach	19 09.5	178 08.8	61.09	0.50	17.35	4.94
ST27	float on beach	19 09.5	178 08.8	58.49	0.71	15.55	5.57
ST28	float on beach	19 09.5	178 08.8	60.15	0.68	17.46	5.22
ST29	float on beach	19 09.5	178 08.8	62.68	0.49	17.36	4.51
ST31	float on beach	19 09.5	178 08.8	58.32	0.71	15.43	5.58

MnO	MgO	CaO	Na2O	K2O	P2O5	LOI	Sc	V
0.08	4.06	6.34	4.62	2.30	0.51	0.45	14	129
0.09	3.93	6.96	4.29	1.90	0.46	1.86	19	198
0.08	3.87	7.26	4.82	1.72	0.56	0.96	14	158
0.07	3.91	5.89	4.66	1.81	0.46	2.91	11	130
0.09	3.75	6.57	4.13	1.60	0.23	1.28	20	178
0.08	3.50	5.89	4.53	1.94	0.30	0.71	14	139
0.08	3.46	6.04	4.75	2.06	0.49	0.83	13	144
0.07	3.37	5.56	4.61	2.03	0.55	1.34	9	108
0.08	3.34	5.56	4.59	2.03	0.34	0.81	14	136
0.07	3.22	6.07	4.39	2.15	0.27	1.20	14	122
0.06	3.23	4.99	4.87	1.86	0.33	0.76	12	116
0.05	3.12	4.97	4.87	2.40	0.36	2.31	13	123
0.08	2.89	5.52	4.59	1.82	0.33	1.54	13	139
0.07	2.75	5.18	4.51	2.23	0.30	1.65	11	108
0.07	2.70	4.44	5.05	2.19	0.38	1.42	8	78
0.07	2.63	4.22	4.89	2.00	0.39	1.71	11	94
0.05	2.56	4.84	5.09	1.46	0.23	1.49	10	97
0.07	2.52	4.49	4.51	2.61	0.28	2.06	11	90
0.07	2.46	5.38	5.23	1.71	0.37	1.16	9	111
0.07	2.27	6.26	4.88	1.78	0.46	1.28	11	133
0.05	2.26	5.36	5.35	1.82	0.38	0.91	10	105
0.06	2.02	3.94	4.30	2.77	0.24	2.49	9	70
0.08	1.10	4.30	5.08	2.13	0.33	1.86	15	115
0.06	2.40	4.32	4.86	1.90	0.33	0.95		
0.08	3.68	6.34	5.01	1.81	0.49	0.94		
0.06	3.30	5.55	4.79	1.97	0.44	1.27		
0.04	1.88	5.22	5.16	1.47	0.24	0.8		
0.06	2.92	5.49	4.73	1.66	0.30	1.56		
0.07	3.26	5.35	4.86	1.65	0.30	0.53		
0.07	2.80	5.48	4.94	1.72	0.37	1.52		
0.04	2.21	5.25	4.75	2.58	0.38	3.1		
0.06	3.15	5.46	4.92	1.92	0.38	3.63		
0.06	3.08	5.89	4.82	1.63	0.22	1.12		
0.08	3.55	6.48	4.24	1.76	0.27	2.53		
0.08	3.13	6.26	4.66	1.55	0.24	4.08		
0.08	3.60	6.15	4.27	1.80	0.23	1.6		
0.12	4.86	7.61	4.39	2.17	0.53	0.93	19	183
0.08	3.47	6.34	4.45	1.78	0.36	1.1		
0.08	2.67	5.39	4.46	2.10	0.25	1		
0.15	5.13	7.71	4.32	2.13	0.52	0.91	19	182

Cr	Ni	Cu	Zn	Rb	Sr	Y	Zr	Nb
97	56			34	1317	10	204	15.5
59	13			7	1263	13	176	8.3
109	114	44	57	23	1580	13	174	12.1
54	48			25	1488	13	191	11.9
15	19			20	888	13	102	3.2
24	22			30	1102	13	132	9.1
56	45			31	1171	16	182	13.8
51	55	41	51	31	1377	14	172	11.3
27	27			32	1151	17	151	10.8
29	25			36	870	15	162	10.0
34	46			29	1048	14	150	9.6
39	29			44	1015	36	164	13.4
12	15			25	1304	29	134	7.6
18	18			34	961	14	175	10.4
21	24			34	909	13	147	9.4
34	38			32	914	13	180	9.9
33	50			17	1120	10	129	5.3
20	19			53	867	12	171	10.7
8	17			23	1136	14	161	9.7
46	32	63	70	23	1667	20	178	8.7
29	28			26	1411	14	171	8.0
16	10	34	38	50	779	16	185	9.9
24	18			34	927	15	152	10.7
140	52	39	62	31	1512	19	182	6.2
139	79	44	99	32	1497	22	180	6.4

Ba	La	Ce	Pr	Nd	Sm	Eu	Gd	Tb
491								
471								
371	33.33	71.83	9.11	34.89	5.83	1.54	3.98	0.51
484								
343								
423								
424								
417	34.48	74.27	9.15	35.42	5.87	1.58	4.08	0.52
453								
459								
412								
483								
536								
490								
414								
409								
402								
567								
413								
466	30.56	64.03	8.74	35.74	6.2	1.75	4.58	0.59
480								
588	28.14	56.64	6.82	25.48	4.46	1.1	3.4	0.49
482								
514	40.30	88.90	11.80	48.70	8.23	2.21	5.59	0.66
537	41.70	96.60	12.80	53.20	9.13	2.43	6.56	0.75

Dy	Ho	Er	Tm	Yb	Lu	Hf	Ta	Pb
2.44	0.44	1.13		0.96	0.14	3.07	0.71	3.6
2.52	0.46	1.2		1.03	0.15	2.36	0.75	5.62
2.99	0.59	1.65		1.6	0.26	3.74	0.5	5.28
2.6	0.52	1.49		1.48	0.23	2.97	0.58	7.56
3.30	0.61	1.60	0.22	1.35	0.22	4.22	0.32	5.53
3.83	0.73	1.99	0.27	1.71	0.29	4.32	0.49	6.48

Th	U
3.94	1.05
5.44	1.91
3.8	1.2
5.36	1.82
4.68	1.41
4.61	1.46